

Tele-Wrist: Development of a 4 DOF End-Effector with Haptic Feedback

Abirami Elangovan¹, Anaya Bhammar¹, Hunsica Jayaprakash¹, Sonali Patel¹

Department of Mechanical Engineering, Department of Biomedical Engineering, Carnegie Mellon University, Pittsburgh, PA, USA

Abstract—Teleoperated surgical robotic procedures assist surgeons in terms of precision and control. However, a primary challenge is the high cost of platforms. The BILK System was developed as a cost-effective alternative, yet faced limitations in terms of limited maneuverability of the end effector and lack of haptic feedback. This reduces the flexibility of procedures capable for the system, as well as removes the tactile aspect of procedures surgeon's have come to rely on. Thus, the need exists for development of an advanced end-effector capable of more intricate procedures and feedback. The Tele-wrist is a 4 DOF system consisting of a Master and Follower wrist. It is capable of mapping a surgeon's wrist motion and opening and closing of a gripper with low latency, within a margin of $\pm 10^\circ$, and providing vibrational feedback on the Master side proportional to force experienced during surgery on the Follower side.

Keywords: Surgical Robotics, Teleoperated surgical system, Real-time robotic control, Haptic Feedback

I. INTRODUCTION

The advent of teleoperated surgical robots marks a significant milestone in surgical technology. These robots, which assist surgeons in performing complex procedures, are known for their precision and control. Central to their design are two main components: the follower arm, inserted into the patient's body, and the master arm, manipulated by the surgeon to control the follower's movements. This innovative technology not only enhances surgical dexterity but also offers a three-dimensional visualization of the operative field [1].

According to Lanfranco et al. (2004), teleoperated surgical robots significantly improve hand-eye coordination and mitigate physiological tremors in surgeons [2]. This advancement is made possible through sophisticated instruments with increased degrees of freedom, allowing for precise tissue manipulation. Additionally, these systems are equipped with hardware and software filters to compensate for surgeon's tremors, a feature critical for delicate procedures.

Research published in the Journal of the American College of Surgeons, notably by Alemzadeh et al. (2016), highlights another crucial advantage: patient safety [3]. The utilization of these robotic systems has been associated with reduced risks of infection and other surgical complications. Moreover, their efficiency can shorten the duration of surgeries, potentially leading to quicker patient recovery.

However, despite these significant advancements, teleoperated surgical robots are not without their limitations.

One of the primary challenges is their high cost [4]. In response to this, the BILK robot was developed as a cost-effective alternative [5]. Yet, it also has limitations, particularly in sensory feedback. While the BILK robot can accurately follow a surgeon's intended trajectory with its scalpel end-effector, it is limited in tool interchangeability, lacks a gripper, and haptic feedback, a critical component for enhancing the surgeon's tactile interaction during procedures [6].

The need for improvement in teleoperated surgical robots is clear. There is a clinical demand for systems that offer greater operational versatility and enhanced surgeon control, especially in delicate surgical contexts where force feedback is vital [7]. Addressing this need, is Tele-Wrist: a revolutionary end-effector featuring four degrees of freedom, haptic feedback, and a modular design. The Tele-Wrist is engineered to overcome the current limitations, aiming to transform the landscape of teleoperated surgical technology and significantly improve surgical outcomes.

II. METHODS

A. System Overview

i. Overview

The system consists of a Master wrist and a Follower wrist. The Master consists of an Inertial Measurement Unit (IMU) connected to a ball joint, and gripper. A surgeon can manipulate the Master wrist. Euler angles for roll, pitch, and yaw (RPY), are collected from the IMU and potentiometer readings are collected from the gripper, coming to 4 Degrees of Freedom (DOF). These are then communicated over an Inter-Integrated Circuit (I2C) connection to control 4 servos on the Follower side to perform the physical operation.

ii. Setup

The Master will only communicate information while the IMU is calibrated. Currently, this requires the gyroscope and magnetometer to be at calibrated values of 3, even if the system overall is not at 3, which has been shown to still provide accurate readings. To calibrate the gyroscope, the Master wrist must be neutral on the calibration stand. Once this has reached 3, the ball joint can be rotated to calibrate the magnetometer. The button can be pressed once the Master is

aligned with the Follower to begin mapping.

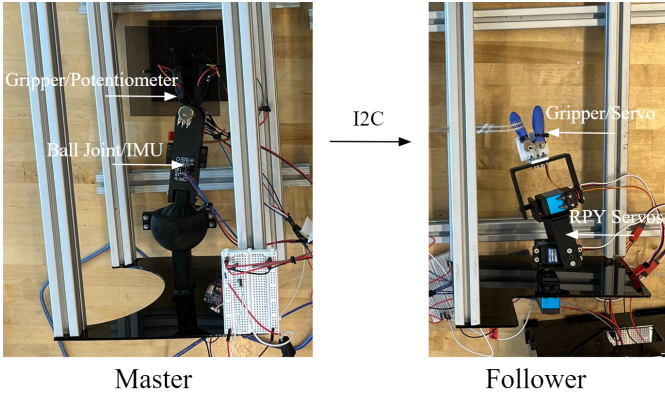


Fig. 1. Overview of Tele-Wrist system.

B. High-Level Hardware

Two Arduino Uno boards were selected, one to control the Master wrist, and one to control the Follower.

C. Communication

The initial proposal included the use of communication between the Master and Follower via HC05 Bluetooth (BT) modules. However, it was found that this resulted in significant latency between readings on the Master side and resulting movements on the Follower side.

Thus, a tethered I2C connection was established, which resulted in reduced latency at a Baud Rate of 115200.

The Arduino Unos were originally chosen as BT connections required Receiving (RX) and Transmitting (TX) connections, and given the other sensors, the Unos provided sufficient pins. However, with the switch to I2C, one set of Serial Data Line (SDL) and Serial Clock Line (SCL) pins were dedicated to tethering the two Arduinos. Thus, given the amount of sensors requiring SDA/SCL connection, the Follower was short one set of pins. As an immediate fix, the Haptic Driver and Force Sensor were both connected to the Master Arduino. However, given different addresses, an I2C bus can differentiate between devices even if all SDA/SCL pins are connected together. This is a matter of choosing the correct pull-up resistors or an I2C module if desired.

D. 3 DOF Wrist Tracking

i. Master - IMU and Roll, Pitch, and Yaw Values

Wrist motion was isolated into Flexion/Extension, Radial/Ulnar Deviation, and Pronation/Supination, depicted in the following figure, with the dotted blue line indicating the neutral position. These can be measured as rotation about Y, X, and Z axes respectively, or pitch, yaw, and roll, totaling three Euler angles.

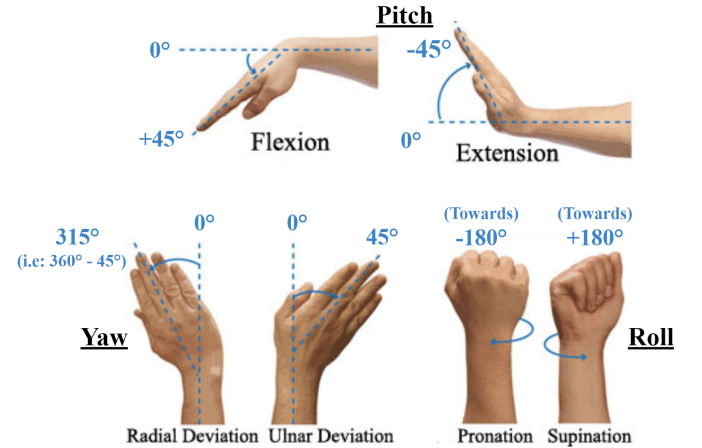


Fig. 2. Summary of isolated wrist motions with example angles, with the dotted blue line indicating the neutral position.

An IMU was desired to track these movements. The three servos on the Follower side were dedicated to creating either the roll, pitch, or yaw motions. Thus, each Euler angle would be passed to their respective servo for the appropriate servo command to be executed. As depicted in Fig. 3, the neutral position for each of the Follower servos is 90°.

Initially, an MPU6050 was utilized. However, this was dismissed as it only combined accelerometer and gyroscope sensors, providing only accurate pitch and roll values, with high yaw drift affecting all readings.

An Adafruit BNO05 sensor was thus selected. This 9 DOF absolute orientation sensor additionally fuses a magnetometer, allowing for more accurate readings. Euler angles were extracted, with the possible range recorded for each as follows, each covering a full rotation of 360° :

TABLE I
RANGE OF EULER ANGLES

Euler Angle	Lower Bound	Upper Bound
Roll	-180°	180°
Pitch	-180°	180°
Yaw	0°	360°

From Fig. 2, as well as user input, it is evident that the range of wrist motion is actually limited to less than 180°. Considering this, along with the controllable range of each servo, the range was restricted:

TABLE II
UTILIZED RANGE OF EULER ANGLES

Euler Angle	Lower Bound	Upper Bound
Roll	-90°	90°
Pitch	-90°	90°
Yaw	0°	180°

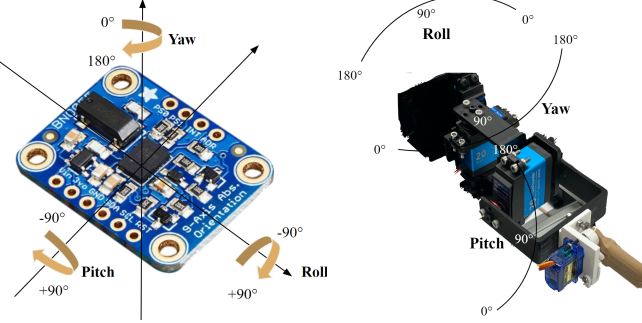


Fig. 3. Roll, Pitch, and Yaw with respect to the IMU and servos.

ii. Master - Yaw Frames

To bring yaw values to the desired range, additional processing was required. It was observed that during new calibrations, the 0° location varied. This was a concern as any value totaling 180° in the $0^\circ \rightarrow 360^\circ$ range could then be the values produced by the IMU. It was thus desired to manipulate the yaw coordinate system, such that 90° always pointed along the neutral axis of the wrist from calibration to calibration.

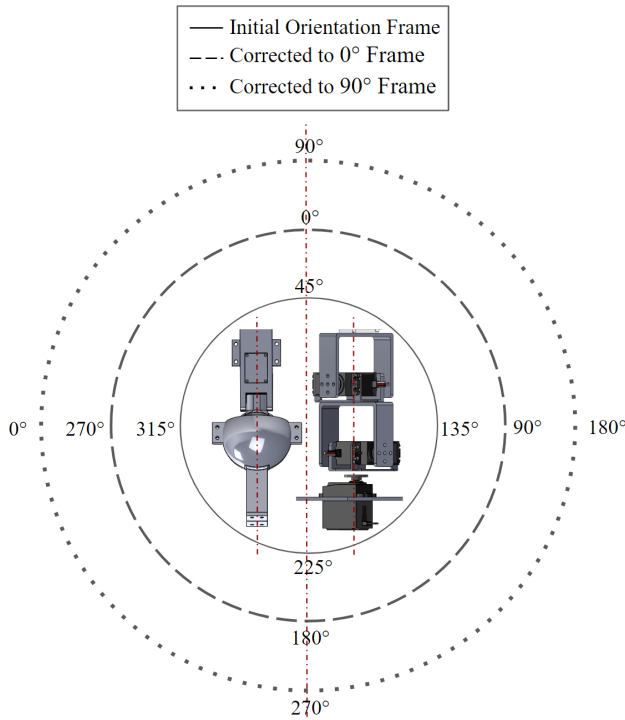


Fig. 4. Depiction of original and corrected yaw coordinate frames, if $\text{yaw}_{\text{initial}} = 45^\circ$ as an example, with dotted red line indicating the neutral axis.

To do this, once the magnetometer was calibrated and the button was pressed, the value was stored as an initial yaw. This was then subtracted from every raw IMU yaw reading. 360° was added if the value became negative. This would shift the coordinate axis such that 0° pointed along the neutral axis, or the Corrected to 0° Frame:

Corrected to 0° Frame

Let initial yaw value = $\text{yaw}_{\text{initial}}$,

Let subsequent yaw readings = yaw ,

Let yaw readings in the 0° Frame = yaw_0 ,

$$\text{yaw}_0 = \text{yaw} - \text{yaw}_{\text{initial}}. \quad (1)$$

If $\text{yaw}_0 < 0$,

$$\text{yaw}_0 = \text{yaw}_0 + 360^\circ. \quad (2)$$

To these values, 90° was added to shift the coordinate axis such that 90° pointed along the neutral axis. The modulo operator was applied to constrain the values to the $0^\circ \rightarrow 360^\circ$ range.

Corrected to 90° Frame

Let yaw readings in the 90° Frame = yaw_{90} ,

$$\text{yaw}_{90} = (\text{yaw}_0 + 90^\circ) \% 360 \quad (3)$$

iii. Master - Mapping

The map() function in Arduino requires an initial value, an initial range the value falls in, and a desired range to map the value into.

After Yaw processing, the mapping was a two-stage process. First, mapping the IMU reading to the 180° servo range. Second, as 270° servos were used, accurately producing the desired angle value from the servo. Normally, this would be a value of $(180 * 180/270) = 120$, but after testing, a value of 130 was found to be more accurate.

$$\text{Roll: } (-90, 90) \rightarrow (0, 180) \rightarrow (0, 130)$$

$$\text{Pitch: } (90, -90) \rightarrow (0, 180) \rightarrow (0, 130)$$

$$\text{Yaw: } (0, 180) \rightarrow (0, 180) \rightarrow (0, 130)$$

The values obtained after the third mapping are the values written to the servo. The IMU to 180° range relationship is depicted in Fig. 3.

As an example, the mapping process for various roll angles is shown below, with the final row being the values written to the servo:

TABLE III
EXAMPLE MAPPING FOR ROLL

IMU Reading	-90°	0°	90°
180° Servo Range	0°	90°	180°
270° Servo Range	0°	65°	130°

iv. Master - Ball and Socket Joint

The IMU was embedded in a mount attached to a ball and socket joint. This was selected as it would allow mimicking natural wrist motion. Design considerations included the semicircular design to achieve the required range of motion. The part was 3D printed from PLA.

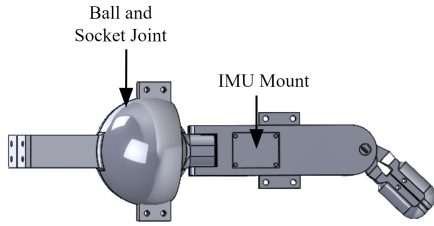


Fig. 5. Master wrist.

v. Follower

The servos selected were SunFounder 20KG High Torque Metal Gear Digital Servo Motors (SF3218MG), with a Control Angle of 270°. These were selected based on the torque specifications that would be required, evaluated below.

The roll servo would be mounted at the base and transmit roll motion to the entirety of the master arm, thus requiring the greatest torque capacity. Required torque was calculated by estimating the weight of the two remaining wrist motion servos, one gripper motion servo, and miscellaneous components, assumed to be acting at the end of the wrist. Servos are often rated in kg cm. A factor of safety of ~2-3 was used for final selection.

TABLE IV
REQUIRED SERVO TORQUE CALCULATIONS

Part	Unit Weight (kg)	Units	Total Weight (kg)	Length (cm)	Torque (kg cm)
High Torque Servo	0.065	2	0.130		8.78
MicroTower Servo	0.009	1	0.009		
Misc.	0.030	1	0.300		
Total			0.439	20	

Modular brackets were designed and 3D printed from PLA. These were designed to allow for any order of mounting of DOF, i.e., interchangeable roll, pitch, and yaw orders. In terms of hardware, M3 heat-set inserts and M3 screws were used.

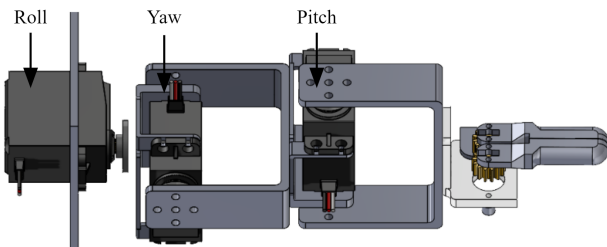


Fig. 6. Follower wrist.

E. 1 DOF Gripper Finger Tracking

i. Master

The Master Gripper was designed to rigidly attach to the ball and socket joint via fasteners. It is a two-part design that houses the IMU, Haptic Driver, and two potentiometers that hold the grippers. The potentiometer detects how wide open the grippers are and is accordingly mapped to the servo on the follower side. There are two finger loops that allow the

surgeon to hold the gripper.

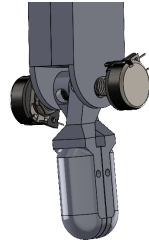


Fig. 7. Master gripper.

ii. Follower

The gripper system on the follower's arm consists of 4 parts: gripper arms, two custom-designed gears, a servo platform, and gripper shelf, and an SG90 9g Microtower servo. The gripper arm design was inspired by laparoscopic tools. The two gears were developed to control the rotational movement of both arms. One is attached to the servo and the other is attached to the gripper platform shelf which allows for opposite rotational movement from both arms when the servo is written to an angle.

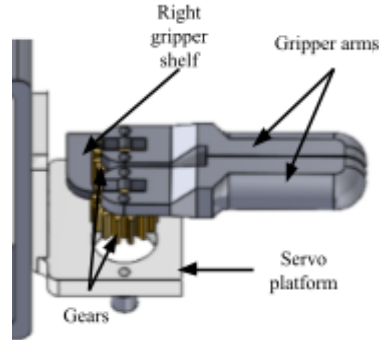


Fig. 8. Follower gripper.

F. Haptic Feedback

The FlexiForce piezoresistive sensor was chosen for the purpose of this project due its flexible nature, small size (for seamless integration on the follower-side gripper), and high accuracy. The force sensor outputs analog values (0-1023) which are converted to voltage values (in mV) and then mapped to haptic sensations through a vibrational motor and a haptic driver, found on the master side. The master haptic driver and vibrational motor interface can be seen in Figure 9 while the force sensor integration with the grippers can be seen in Figure 10. The motor has capabilities of clicks, ramps, buzzes, and pulses. After testing out multiple motions of the motor, pulses were chosen as the haptic sensation for continuous feedback to the surgeon. As the force detected by the sensor increases, the pulses amplify and vice versa.

$$\text{Voltage} = \text{Analog Value} * (5/1023) \quad (4)$$



Fig. 9. Master haptic driver and vibrational motor interface.



Fig. 10. Follower force sensor.

G. Power Supply

Each 4.8-7.2V servo was estimated to draw 1A at 5V, with roll drawing the most due to it having the greatest load torque, and pitch the least due to having the least load torque. Thus, three power supplies were utilized - three 9V batteries, each connected to an HW 131 breadboard power supply to step down to 5V as seen in Fig 11. Roll and yaw were powered through their own designated power supplies, and the pitch was consolidated with remaining sensors and drivers. The MicroTower servo was powered from the 3.3 V pin of the Follower Arduino.

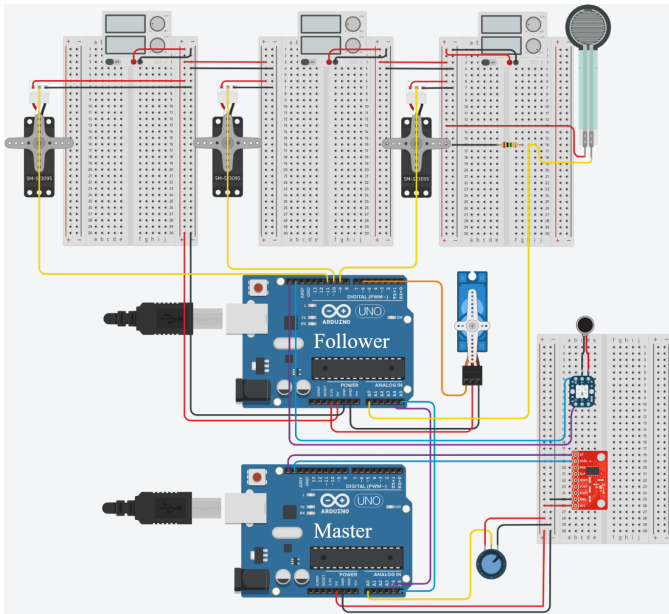


Fig. 11. Master and Follower wrist circuit diagram.

H. Evaluation Experiments

Three tests were performed for the evaluation of the Tele-Wrist system. First, the positional accuracy of the servos was evaluated. Secondly, the ease of maneuverability and the translation of the master-to-follower gripping function were

evaluated by implementing a ring toss activity. Thirdly, haptic feedback from the force sensor on the follower's arm to the master's arm was assessed for the user's sense of interaction.

i. Evaluation 1: Position Accuracy

The first assessment evaluated the error in IMU and master position-to-follower mapping. The master and follower arm's roll, pitch, and yaw angles were documented for a range of angles at each orientation. The maximum angles of each orientation were recorded along with three random angles between the maximum. The maximum angles were defined as the greatest angle from the center axial zero line of the arm that the master was capable of reaching. To attain these errors, the system was turned on, IMU was calibrated, and then the master arm was directed in an orientation. A digital angle gauge was used to measure the angles of the follower and master arms, while an iPhone compass was used to measure the yaw of the arms. The original and mapped angles recorded can be found in Tables V, VI, & VII.

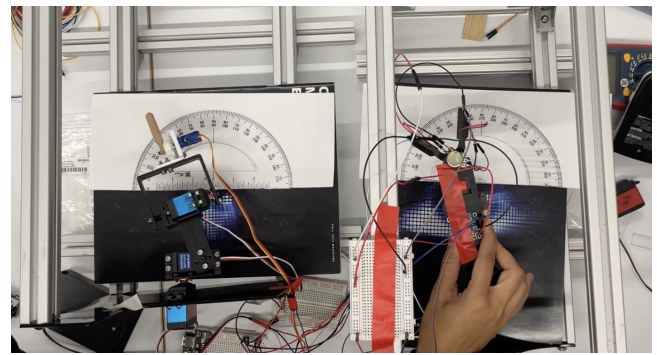


Fig. 12 . Position Accuracy Test for the range of motion of yaw

ii. Evaluation 2: Maneuverability and Grip

The second test consisted of evaluating the maneuverability and gripping of the system using a ring toss assessment. Three users, one with experience with the system and two new users, were timed and tasked with placing three rings on three separately positioned rods on a platform using the master arm. Times were recorded from the second the follower gripper was given the ring to the time the user placed the last ring on the last rod, as seen in Table VIII. This activity also investigated the maximum range of the arms.

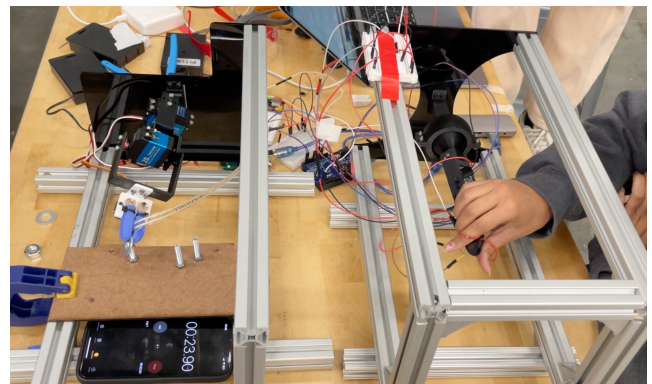


Fig. 13. Maneuverability and Grip Ring Toss Test.

iii. Evaluation 3: Haptic Feedback

A stiffness test was performed to determine whether the haptic feedback could inform the surgeon of stiffer materials. The two materials used were Polyolefin ($E = 2.5\text{Gpa}$) and Clay ($E = 8.0\text{Gpa}$) of comparable thicknesses. The user then attempted to squeeze the materials to their max ability using the gripper and the maximum analog output was recorded in Table IX.

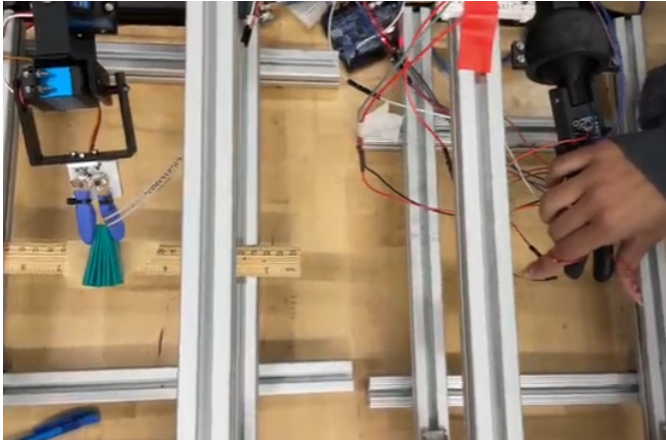


Fig. 14. Haptic Feedback Stiffness test with Polyolefin.

Although tests were carried out by recording analog values, it was desired to convert these to force values for complete understanding. The analog output of the FlexiForce sensor was recorded across a spectrum of known applied weights. Surgical practices typically involve maximum forces on the order of 0.04N in Ophthalmology, 0.4N for Nervous Tissue, and 0.03N for sharp dissections [8]. Consequently, forces applied in this experiment were capped at 0.8N. Eq. 4 was used to convert the analog values to voltage. These were then plotted against the known applied forces in Fig. 15.

III. RESULTS

Position accuracy, maneuverability and grip, and haptic feedback results from the evaluation tests of the master and follower integration can be seen in the following sections.

A. Results 1: Positional Accuracy

TABLE V

POSITION ACCURACY: ROLL

IMU Euler Angle	Observed Master Angle	IMU Euler Angle and Observed Master Angle $ \Delta^\circ $	Observed Follower Angle	Observed Master Angle and Follower Angle $ \Delta^\circ $
90°	89°	1°	86°	3°
48°	49°	1°	47°	2°
-40°	-37°	3°	-36°	1°
-52°	-56°	4°	-52°	4°
-74°	76°	2°	-76°	0°

TABLE VI

POSITION ACCURACY: PITCH

IMU Euler Angle	Observed Master Angle	IMU Euler Angle and Observed Master Angle $ \Delta^\circ $	Observed Follower Angle	Observed Master Angle and Follower Angle $ \Delta^\circ $
38°	-40°	2°	-40°	0°
31°	-31°	0°	-31°	0°
-22°	22°	0°	20°	2°
-29°	36°	7°	28°	8°
-37°	43°	6°	36.5°	6.5°

TABLE VII

POSITION ACCURACY: YAW

IMU Euler Angle 198° Heading	Observed Master Angle 270°	IMU Euler Angle and Observed Master Angle $ \Delta^\circ $	Observed Follower Angle	Observed Master Angle and Follower Angle $ \Delta^\circ $
251°	29°	24°	37°	8°
239°	49°	8°	41°	8°
221°	19°	4°	22°	3°
172°	29°	3°	30°	1°
169°	43°	6°	33°	10°

B. Results 2: Maneuverability and Grip

TABLE VIII

MANEUVERABILITY AND GRIP: RING TOSS

User	Time (seconds)
User 1 (Experienced User)	38
User 2 (New User)	69
User 3 (New User)	75

C. Results 3: Haptic Feedback

TABLE IX

MAX COMPRESSIVE FORCE FOR DIFFERENT MATERIALS

Material	Elastic Modulus (GPa)	Thickness	Max Analog Reading	Haptic Vibration Level
Polyolefin	2.5	5.188	153	3
Clay	8.0	5.125	212	4

The voltage versus force data was subjected to a curve fitting analysis, and the logarithmic relation emerged as the most suitable fit, supported by the highest observed R^2 value of 0.985.

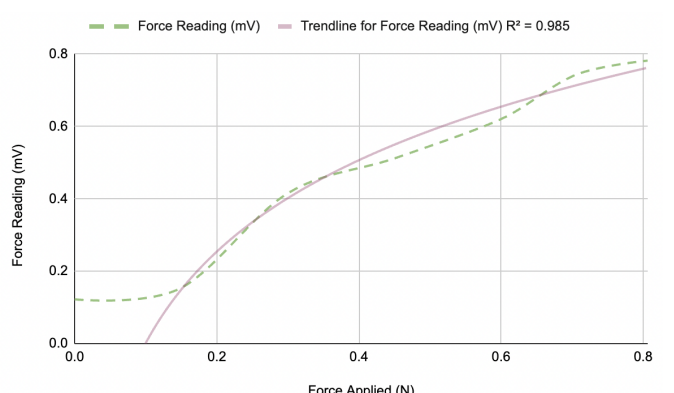


Fig. 15. Force Output vs Force Applied on FlexiForce Sensor

IV. Discussion

A. Evaluation Test Discussion

For Evaluation 1, the IMU and follower were able to successfully mimic roll, pitch, and yaw of the master with roll having an error of ± 4 degrees, pitch with an error of ± 6 degrees, and yaw with an error of ± 11 degrees, as can be seen in Tables V, VI, and VII. The roll orientation had the highest position accuracy. This may be because the servo controlling the roll of the arm is in the most stable position as it is fixed in the middle of the system and was measured around a stable axis point. Yaw had the lowest position accuracy which could be attributed to the accumulated drift over time in the yaw orientation. Moreover, while measuring the angles in the pitch direction, an offset was implemented and subtracted from the angle measured as a tilt in the pitch axis was observed, likely due to the arm's weight and the brackets' flexibility allowing for deformation.

For Evaluation 2, the maneuverability activity allowed for testing of the mobility of servos at once including the gripper servo. The first user, the one with the most experience completed the task the fastest. This was likely because the first user was the most familiar with the controls of the system. Overcoming the learning curve of the system can benefit the performance during mobility activities. However, some limitations include that the system was only tested on three users. Testing the system with users of varying experiences can help uncover how mobility can be improved. Additionally, the initial code of the system instructed the follower arm to halt when IMU calibration values were not met. Throughout testing, this caused a delay in the task completion as the follower servos would stop moving. Moreover, this caused a loss of secure grip from the follower on the rings which resulted in the gripper dropping the rings. The range would be improved with integration with the BILK.

For Evaluation 3, a stiffness test with Polyolefin and clay further explored haptic feedback's effectiveness. The stiffer material (clay) outputted higher compressive forces and stronger haptic vibrations at the master, proving the benefit of real-time haptic feedback. This confirmed the system's ability to convey real-time haptic feedback effectively, with stiffer materials generating higher compressive forces and stronger vibrations, underscoring the system's utility in differentiating material stiffness.

The sensor was also analyzed using various known applied weights, reflecting real surgical force applications in various procedures. Forces were limited to 0.8N. The results, plotted on a graph against voltage, were analyzed through curve fitting. A strong logarithmic relationship with a high R^2 value was shown, indicating a strong correlation between force and voltage.

Thus, as the force applied increases, the corresponding voltage increases at a diminishing rate. Accordingly, the haptic vibrations were mapped where the vibration intensity experiences a more rapid increase in frequency at lower force values. As the applied forces rise, the intensity continues to increase, but the rate of this increase diminishes, occurring

with reduced frequency as forces reach higher levels. Thus, haptic vibration levels ranged from 1-5, with 1 being the lowest intensity.

B. Future Work

In order to enhance the future development of the Tele-Wrist system, efforts will be focused on refining its mechanical and electrical integrity, along with improving communication technology. This aligns with the clinical demand for more advanced teleoperated surgical robots that offer superior operational versatility in end-effectors, modular gripper designs, and precise surgeon control [9]. Key mechanical improvements will include bolstering servo brackets, optimizing gripper motion, and enhancing gripper friction to prevent slipping. On the electrical front, upgrades like a larger initial supply with separate voltage converters for the high-torque servos will be used. The Alorium XLR8 Board will be integrated to increase servo smoothness. Furthermore, Bluetooth technology will be further experimented with and implemented to ensure seamless communication between the master and follower arms.

Additionally, it should be noted that the Tele-Wrist was designed for integration with the BILK system, strictly to accurately map Euler angles. With the current set-up, roll, pitch, and yaw do occur around one axis, however, pitch will have an x-y offset due to being mounted further down the wrist, and angle mapping not occurring from the point where roll is attached to the base. For integration with the BILK, having both pitch and yaw result in a redundant DOF. Removing one of these resolves the redundancy and offset problems, an easy task given the modular design.

Collectively, these enhancements, coupled with the Tele-Wrist's innovative four-degree freedom design and sophisticated haptic feedback within a modular framework, aim to revolutionize teleoperated surgical procedures, offering surgeons tools designed for the complexities of modern surgeries.

REFERENCES

- [1] F. Cepolina and R. P. Razzoli: "An introductory review of robotically assisted surgical systems," *Int. J. Med. Robot.*, vol. 18, no. 4, Art. no. e2409, Aug. 2022, doi: 10.1002/rcs.2409. Epub 2022 May 4. PMID: 35476899; PMCID: PMC9540802.J.
- [2] A. R. Lanfranco, A. E. Castellanos, J. P. Desai, and W. C. Meyers: "Robotic surgery: a current perspective," *Ann. Surg.*, vol. 239, no. 1, pp. 14-21, Jan. 2004, doi: 10.1097/01.sla.0000103020.19595.7d. PMID: 14685095; PMCID: PMC1356187
- [3] H. Alemzadeh, J. Raman, N. Leveson, Z. Kalbarczyk, and R. K. Iyer: "Adverse Events in Robotic Surgery: A Retrospective Study of 14 Years of FDA Data," *PLoS One*, vol. 11, no. 4, Art. no. e0151470, Apr. 2016, doi: 10.1371/journal.pone.0151470. PMID: 27097160; PMCID: PMC4838256.
- [4] A. Mohan, U. U. Wara, M. T. Arshad Shaikh, R. M. Rahman, and Z. A. Zaidi: "Telesurgery and Robotics: An Improved and Efficient Era," *Cureus*, vol. 13, no. 3, Art. no. e14124, Mar. 2021, doi: 10.7759/cureus.14124. PMID: 33927932; PMCID: PMC8075759.
- [5] D. G. Shankar, R. Singhal, S. Bharadwaj, and S. Mohanraju, "Enhancement Of The BILK Robot Platform," in Proc. Carnegie Mellon University, Medical Robotics, Pittsburgh, PA, US, 2022, pp. 1-2
- [6] R. Babik, J. Inacio, L. Kesavan, and C. Lin, "Development of a Tele-Operated Surgical System BILK," Department of Mechanical Engineering, Biomedical Engineering and Robotics, Carnegie Mellon

University, Pittsburgh, PA, US, 2021, Medical Robotics, Carnegie Mellon University.

- [7] L. Kuang, M. Ferro, M. Malvezzi, D. Prattichizzo, P. Robuffo Giordano, et al.: "A Wearable Haptic Device for the Hand with Interchangeable End-Effectors," IEEE Transactions on Haptics (ToH), vol. 2023, Special Issue on "Haptics in the metaverse: Haptic feedback for Virtual, Augmented, Mixed, and eXtended Realities," pp. 1-10, 2023, doi: 10.1109/TOH.2023.3284980. HAL: hal-04122655.
- [8] Golahmadi AK, Khan DZ, Mylonas GP, Marcus HJ. Tool-tissue forces in surgery: A systematic review. Ann Med Surg (Lond). 2021 Mar 31;65:102268. doi: 10.1016/j.amsu.2021.102268. PMID: 33898035; PMCID: PMC8058906.
- [9] A. Balaji et al.: "Design and Analysis of Universal Gripper for Robotics Applications " in IOP Conf. Ser.: Mater. Sci. Eng., vol. 1012, no. 012006, 2021.